Changes in Metal Transfer Behavior during Shielded Metal Arc Welding

Basic, cellulose and rutile covered electrodes showed significant changes in transfer characteristics as they were consumed

BY P. G. H. PISTORIUS AND S. LIU

ABSTRACT. The transfer of metal droplets during shielded metal arc welding was studied. Cellulose, rutile, basic electrodes and a rutile covered stainless steel electrode were used. The transfer behavior was characterized by analysis of the arc signal, by plotting the welding voltage histogram, and by calculating the frequency response of the welding voltage. Some nonfusion welds were made using rutile electrodes. The size distribution of the droplets could be correlated with the arc signal. The metal transfer behavior generally changed significantly as the electrode was consumed. These changes were larger if the welding current was higher. The transfer behavior of the stainless steel electrode has the lowest sensitivity to changes in the welding current.

Introduction

In this work, the transfer of metal droplets during shielded metal arc welding is investigated. Most of the published work on transfer behavior during arc welding involves gas metal arc welding or flux cored arc welding. The fundamental principles of the characterization of metal transfer behavior are similar for most consumable electrode welding processes. Previous work on gas metal arc welding and flux cored arc welding will therefore be discussed.

Metal Transfer in Gas Metal Arc and Flux Cored Arc Welding

Most studies on the metal transfer behavior during arc welding characterize the gas metal arc welding process. Heald, *et al.* (Ref. 1) studied the droplet transfer modes during gas metal arc welding with a 1.2 mm (0.047 in.) diameter AWS ER100S-1 electrode. An Ar-2%O_2 shielding gas was used. The DC power source provided a constant voltage. The transfer behavior was characterized using various techniques. Laser backlighted photography was used to generate high speed video images of the transferring droplets, and voltage and current fluctuations were measured. Three transfer modes were considered, namely, short circuit transfer, globular transfer, and spray transfer. The standard deviation of the welding current was useful to establish whether spray transfer occurred. However, the standard deviation of the welding current could not be used to reliably distinguish between globular and short circuit transfer.

Modenesi and Nixon (Ref. 2) studied arc instability during the initial stages of a gas metal arc weld. Various shielding gases were used. Most of the welding was done with a constant current power supply. The welding voltage varied between three levels: the short circuit voltage, an intermediate voltage, which was associated with stable operation, and a high voltage, associated with unstable operation. The arc instability could be gauged by plotting the histogram of the welding voltage. Unstable operation was associated with a histogram exhibiting three peaks, corresponding to these three voltages.

KEY WORDS

Metal Transfer
Shielded Metal Arc
Covered Electrodes
SMAW
Arc Signal
Stainless Steel
Cellulose
Rutile

Jönsson, *et al.* (Ref. 3) characterized the voltage and power distributions in gas metal arc welding with an extensive experimental and numerical study. The experimental work was done using an 1.14 mm (0.045 in.) diameter ER100S-1 electrode with a 95% argon – 5% carbon dioxide shielding gas. The welding current varied between 200 and 326 A. The total voltage measured between the contact tube and the workpiece was the sum of the voltage drop at the contact resistance between the contact tube and the electrode, the voltage drop in the electrode extension, and the arc voltage. The arc voltage dominated the total measured voltage, confirming the results of an earlier theoretical study (Ref. 4). It was found that the voltage drop in the electrode extension was a significant fraction of the total voltage only if a high-resistivity electrode, such as stainless steel, was used.

Metal transfer in flux cored arc welding was characterized by Wang, *et al.* (Ref. 5) for a wide range of welding current and voltage. An AWS E71T-1 1.6 mm diameter electrode was used, with a 75% argon – 25% carbon dioxide shielding gas. A constant voltage power supply was used. A range of techniques was used to characterize the transfer behavior. Welding on a water cooled copper tube over a water bath made droplet collection possible. The size distribution of these droplets was measured by image analysis. A fast Fourier transform of the welding voltage was used to identify dominant frequencies. Voltage fluctuations were counted and classified by their magnitude. The results of these techniques could be correlated. The transfer behavior of flux cored arc welding under

P. G. H. PISTORIUS is with the Department of Materials Science and Metallurgical Engineering, University of Pretoria, Pretoria, South Africa. S. LIU is with the Metallurgical and Materials Engineering Department, Colorado School of Mines, Golden, Colorado.

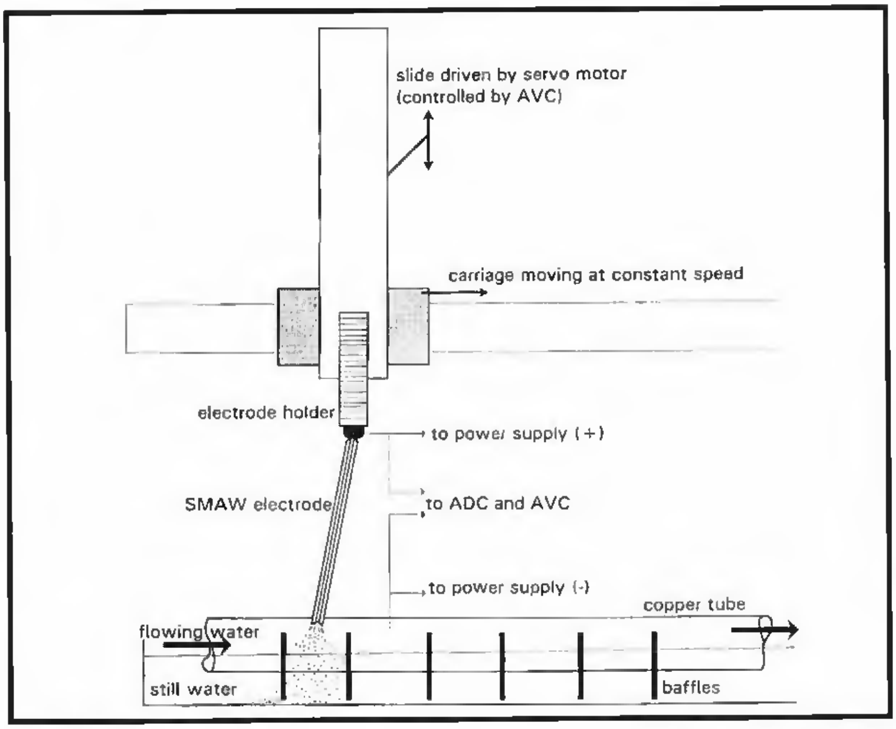

Fig. 1 — Schematic view of experimental apparatus used to weld on a water-cooled copper tube. AVC: arc voltage controller; ADC: analog-to-digital card. The same apparatus was used to prepare bead-on-plate welds.

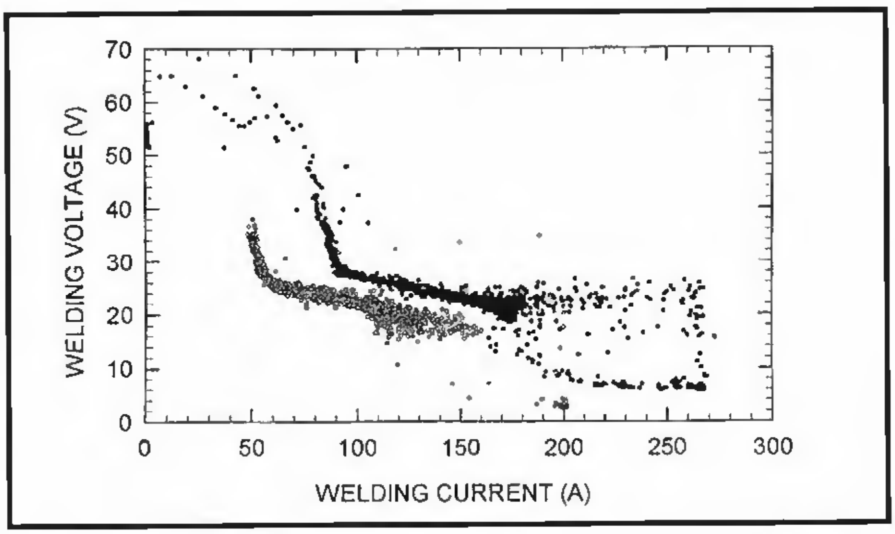

Fig. 2 — Voltage – current characteristic of the power supply, as determined during welding with an E7018 electrode at 96 A (open symbols), and at 150 A (closed symbols).

the specific conditions was usually a mixture of short-circuiting, globular and spray transfer. Pure spray transfer was never observed.

Recent work on the characterization of metal transfer behavior in gas metal arc welding and flux cored arc welding indicates that the arc signal can be used to characterize the metal transfer behavior. The choice between the use of the welding current or voltage depends on the type of power supply used. If a constant current power source is used, it is customary to use the voltage between the contact tube and the workpiece to characterize the transfer behavior.

Metal Transfer in Shielded Metal Arc Welding

Shielded metal arc welding differs from both gas metal arc welding and flux cored arc welding in that it is an inherently transient process. Furthermore, as with FCAW, the presence of a molten slag affects the transfer behavior fundamentally.

One of the first studies on the effect of the heating of the electrode on the welding behavior of shielded metal arc welding electrodes was done by Stern (Ref. 6). An increase in both the electrode length and the welding current would increase the heating of the electrode. Cellulose electrodes 5.6 mm (7/32 in.) in diameter were resistively heated by a current which varied between 180 and 280 A. The associated increase in temperature was only due to resistance heating of the metal core; no welding arc was present. During welding, the electrode temperature at a specific point was approximately equal to the temperature of the resistively heated electrode, until the arc was within 13 mm of that point. These results would indicate that resistive heating of the electrode constitutes a larger contribution to the heating of the electrode than conduction from the arc. The amount of resistive heating was sensitive to the resistivity of the metal, the change in the resistivity with temperature, and the current density. As a first approximation, therefore, the current density can be used to compare the results of different studies, where electrodes with different diameters were used. (In this paper, the current density was expressed as the welding current divided by the cross sectional area of the electrode, excluding the diameter of the flux covering.) Stern (Ref. 6) varied the current density between 7.4 and 11.5 A/mm^2.

Ter Berg and Larigaldie (Ref. 7) studied the factors governing the melting rate and transfer behavior of shielded metal arc welding electrodes. The increase in temperature of the electrode, as well as the influence of the welding current on the size of this increase in temperature were demonstrated. The increase in temperature of the electrode was again attributed to resistance heating. One of the implications of the heating of the electrode was that the specific melting rate increased as the electrode was consumed. Ter Berg and Larigaldie also quoted previously published measurements of the weight of drops generated by direct current welding with bare electrodes. A higher welding current density favored transfer by smaller droplets. For a fixed electrode diameter, the absolute melting rate increased with the welding current. If the droplet diameter decreases at the same time, the number of transfer events should increase with an increase in the current. Higher frequencies would therefore become more dominant as the welding current was increased.

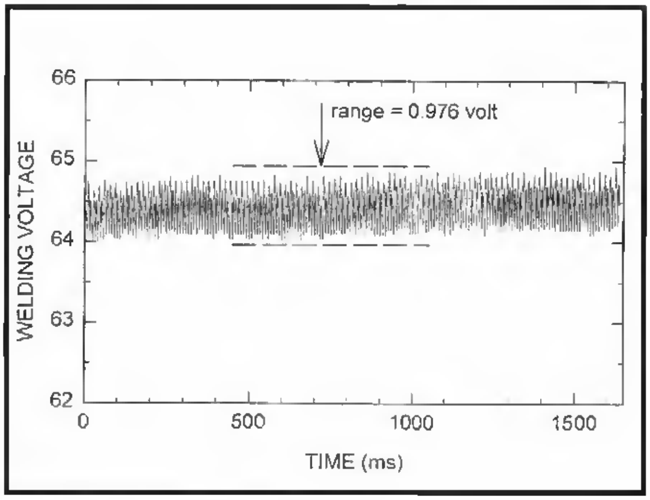

Fig. 3 — Voltage signal with an open circuit.

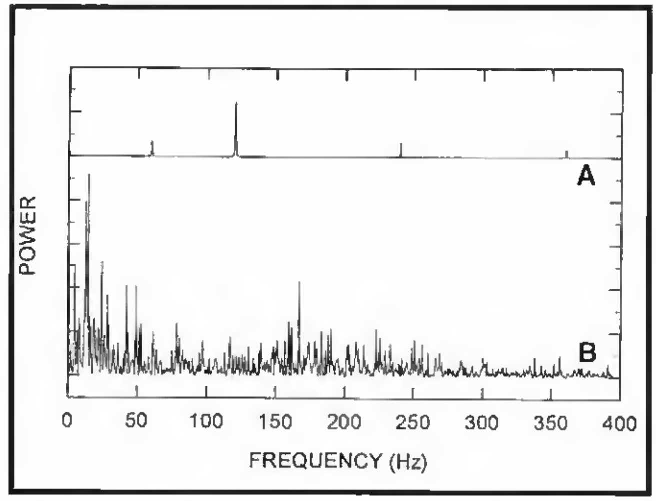

Fig. 4 — A — Power spectrum of the open circuit voltage signal, as determined by fast Fourier transform. B — The fast Fourier transform of the welding voltage signal, shown with the same vertical scale as A.

The melting rate, and the factors that govern the melting rate, were further investigated by Waszink and Piena (Ref. 8). E6013 (rutile), E7024 (rutile – iron powder), and E7016 (low hydrogen – potassium) electrodes were used. The experimental welds covered a broad range of current density, from 2.6 A/mm^2 to almost 19 A/mm^2 for E6013 electrodes. For E7024 electrodes, the current density ranged from 12 to 25 A/mm^2. For E7016 electrodes, the corresponding figure was 9 to 20 A/mm^2. An analytical model for the molten length of electrode, as a function of time, was developed. This model accounted for heating of the electrode by conduction heat transfer from the molten droplet, but not for ohmic heating of the electrode core. The model could predict the molten length to within a few percent of the experimental measurements. The use of this model to predict the length of electrode consumed was demonstrated for an E7016 (low hydrogen – potassium) electrode. The discrepancy between the model prediction and the actual length of electrode consumed was never more than about 6%. Based on these results, the authors claimed that most shielded metal arc welding was done at a current range where ohmic heating of the electrode core was not significant.

Heating of the electrode, and the flux, may result in changes in the chemical composition of the electrode covering. This aspect was investigated by Chen and Kang (Ref. 9). A $CaCO_3$ based flux was heated in a furnace, through the thermal cycle corresponding to that encountered by the electrode, near the electrode holder. Very little CO_2 was generated during heating up to about 300°C (572°F). The authors claimed that this temperature corresponded to a welding time of about 60 seconds. (No indication of the assumed welding current was given.) Heating to higher temperatures results in the evolution of substantial amounts of CO_2 from the flux. Chen and Kang also measured the change in the chemical composition of the weld metal, by measuring the manganese, silicon, and oxygen content of individual droplets. Initial ignition of the arc was associated with significant changes in the chemical composition of droplets. Oxygen showed a peak of about 1000 ppm, followed by a drop to about 600 ppm. At the same time, the Mn and Si content increased monotonically. The transient period lasted about 600 ms from the time the arc was first ignited.

Three metal transfer modes were active during shielded metal arc welding (Ref. 10). These modes were: transfer by large droplets (short circuit transfer), explosive transfer, and fine droplet transfer. Short circuit transfer occurred with basic electrodes, and all other electrodes when welding at low currents. Explosive transfer was characterized by the random separation of droplets from the liquid metal at the tip of the electrode, and occurred with organic coatings. Rutile coatings, when used at conventional current densities, exhibited fine droplet transfer. When welding with a rutile electrode, heating of the electrode resulted in an increase in the size of the droplets. The transfer mode could be characterized using a range of techniques, such as the use of a fast Fourier transform of the arc signal to identify the dominant frequencies, plotting the distribution of the actual welding voltage or welding current, and by calculating the short circuit time. Of these techniques, the use of the short circuit time was favored. Neither the standard deviation nor the variance of the instantaneous value of the welding voltage was recommended (Ref. 11). When using a rutile electrode, a large number of small droplets detached from the electrode tip. Every time a droplet detached from the tip of the electrode, the welding voltage increased. The number of changes in the welding voltage was therefore large when using a rutile electrode, and the variance was large. When using basic electrodes, the welding voltage fluctuated over a wider range. However, there was a smaller number of changes in the welding voltage, and a lower variance of the welding voltage. They concluded that the variance of the welding voltage did not give a reliable indication of the transfer mode in shielded metal arc welding.

The metal transfer behavior during shielded metal arc welding was studied for E6011 (cellulose), E6013 (rutile) and E7018 (low hydrogen) electrodes by Brandi and coworkers (Ref. 12). The current density ranged from 7.6 A/mm^2 to 15.9 A/mm^2. Three metal transfer modes were identified: explosive, short circuit, and slag guided transfer. The transfer mode was characterized by welding on a rotating copper disk, collecting the droplets in water, and screening the droplets. The size distribution of the droplets was reduced to a single figure, the characteristic diameter. This figure

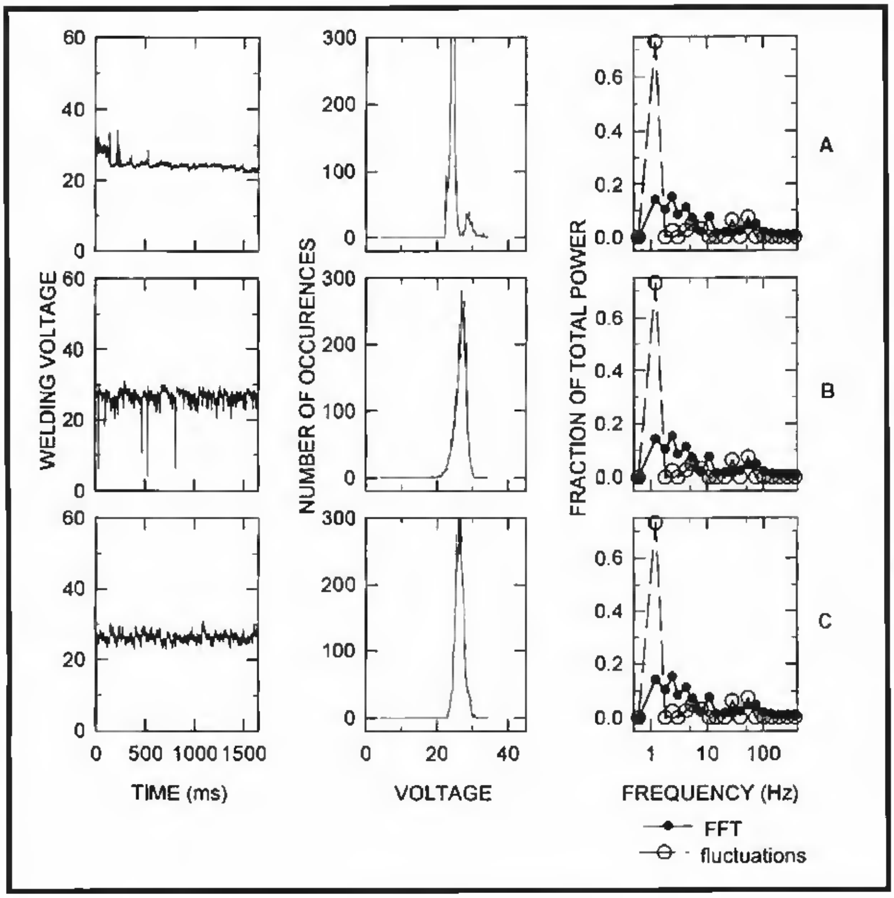

Fig. 5 — Change in behavior as a rutile electrode (E6013) is consumed during welding on a water-cooled copper tube, as exemplified by the welding voltage signal, the histogram of the welding voltage, and the frequency response. The frequency response is calculated by summarizing the results of the fast Fourier transform (•), and the size of the individual fluctuations in the welding voltage (o). Welding current 129 A; recommended current range 120 to 135 A. A — Behavior during the initial 1.6 s of welding. B — Behavior after approximately 11 s of welding. C — After 35 s. The total arc time was about 40 s.

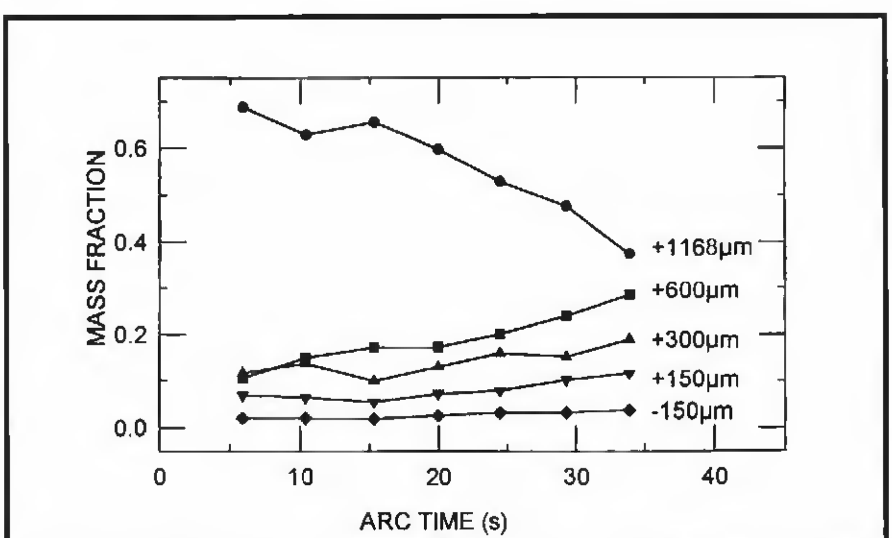

Fig. 6 — The size distribution of droplets captured in a water bath during welding with a rutile electrode on a copper tube. Welding current: 129 A; the corresponding welding voltage signal is shown in Fig. 5.

was used to calculate the apparent density and the porosity of the droplets. Metallographic results showed that droplets smaller than 1 mm (0.039 in.) did not have any porosity. The amount of spatter was quantified by the number of droplets between 500 μm (0.020 in.) and 212 μm (0.008 in.). The rutile electrode had the lowest amount of spatter. E7018 showed a slightly higher amount of spatter. A change in polarity, from DCEP to DCEN, or the use of a higher welding current, resulted in a smaller characteristic diameter and more spatter. Increasing the diameter of the core wire, without adjusting the welding current, increased the characteristic diameter and reduced the amount of spatter. Explosive transfer was characterized by a smaller characteristic diameter and a broad size distribution.

The collection of droplets in a water bath was also used to study the change in transfer behavior and the chemical composition of the weld pool as a shielded metal arc welding electrode was consumed (Ref. 13). Three electrode types — E6013, E7018, and E12018 — were used at a welding current of around 134 A. The current density was just below 17 A/mm^2. E7018 electrodes were also welded with a current of 100 and 150 A (12.6 and 18.9 A/mm^2). As the electrode was consumed, the droplet size increased. An increase in droplet size was associated with an increase in the manganese and silicon content of the weld pool, and a reduction in the oxygen content. The resultant change in the chemical composition along the weld bead appeared over a much coarser scale than the change in chemical composition demonstrated by Chen and Kang (Ref. 8). The changes in transfer behavior, and in chemical composition along the weld bead, were more pronounced if a higher welding current was used.

In related work, Bracarense and Liu (Ref. 14) reported on the influence of the chemical composition of the covering of basic electrodes on electrode heating. A bare electrode, a commercial E7018 electrode, and three experimental electrodes containing 20% calcium carbonate – $CaCO_3$, 20% dolomite – (Ca, Mg) $(CO_3)_2$, and 10% $CaCO_3$ plus 10% dolomite, respectively, were used. The uncoated electrode had a considerably higher melting rate, as no heat was necessary for the melting of the electrode coating. The temperature of the uncoated electrode close to the electrode holder increased more rapidly as the electrode was consumed. The dolomite containing electrodes had the same melting rate as the calcium carbonate electrodes, for a

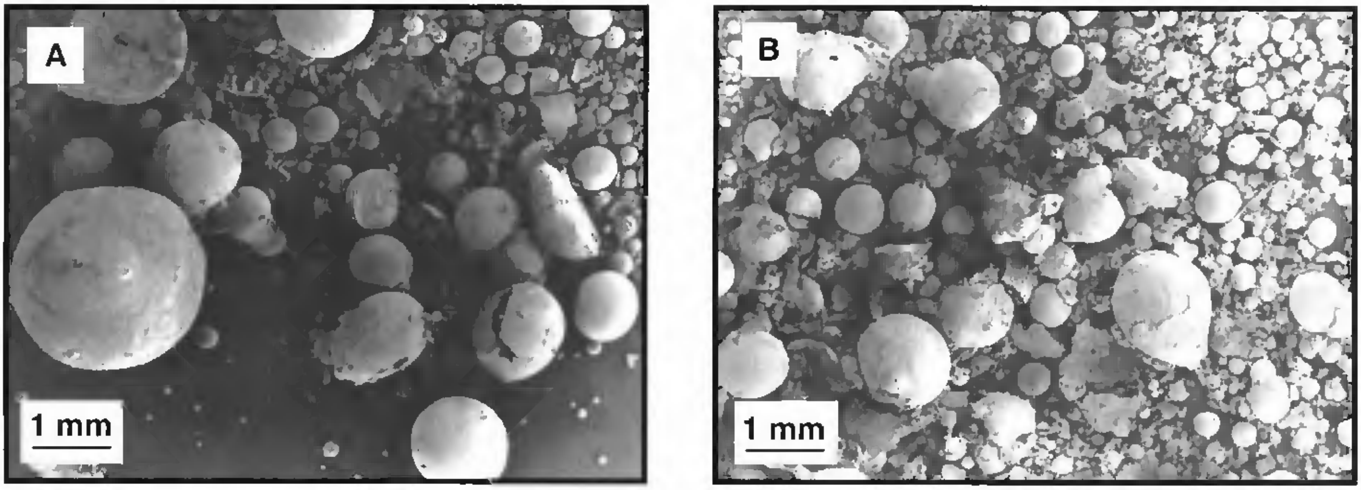

Fig. 7 — Some of the droplets collected during welding with a rutile electrode on a water-cooled copper tube. The corresponding welding voltage signal is shown in Fig. 5; the size distribution of all the collected droplets, in Fig. 6. A — Arc time 6 s. B — Arc time 34 s. Note the increase in the number of small droplets with a longer arc time.

welding current of 100A. The peak temperature reached under these conditions was below the decomposition temperature of $CaCO_3$ (894°C) (1640°F). Therefore, the endothermic decomposition reaction of the $CaCO_3$ in the electrode coating did not occur until very close to the arc, and this reaction did not limit the increase in the electrode temperature. In the electrode containing 20% dolomite, the decomposition of $MgCO_3$ may help to limit the increase in electrode temperature. The peak temperature at a distance of 250 mm (9.8 in.) from the tip, for the dolomite containing electrode, was about 630°C (1166°F), which was some 60°C (140°F) lower than the corresponding figure for the electrode containing no dolomite. This phenomenon was explained by the lower decomposition temperature of $MgCO_3$ (314°C [597°F]), in contrast to 894°C [1640°F] for $CaCO_3$), and the higher thermal conductivity and heat capacity of dolomite.

In summary, shielded metal arc welding exhibits three transfer modes: short circuit, explosive, and slag-guided transfer. As with flux cored arc welding, some of these transfer modes can be present simultaneously. In basic electrodes, short circuit transfer dominates. Welding with a higher current results in a smaller droplet size. When welding a basic electrode, the droplet size increases as the electrode was consumed (Ref. 12). This was probably due to the heating of the electrode, and the associated changes in the chemistry of the flux. The extent of these changes may be reduced by using an electrode coating containing dolomite. The electrode was heated by ohmic heating, and by heat transfer from the molten drop at the tip of the electrode. Ohmic heating is dominant far away from the molten tip. The contribution from both these mechanisms increases with a higher welding current.

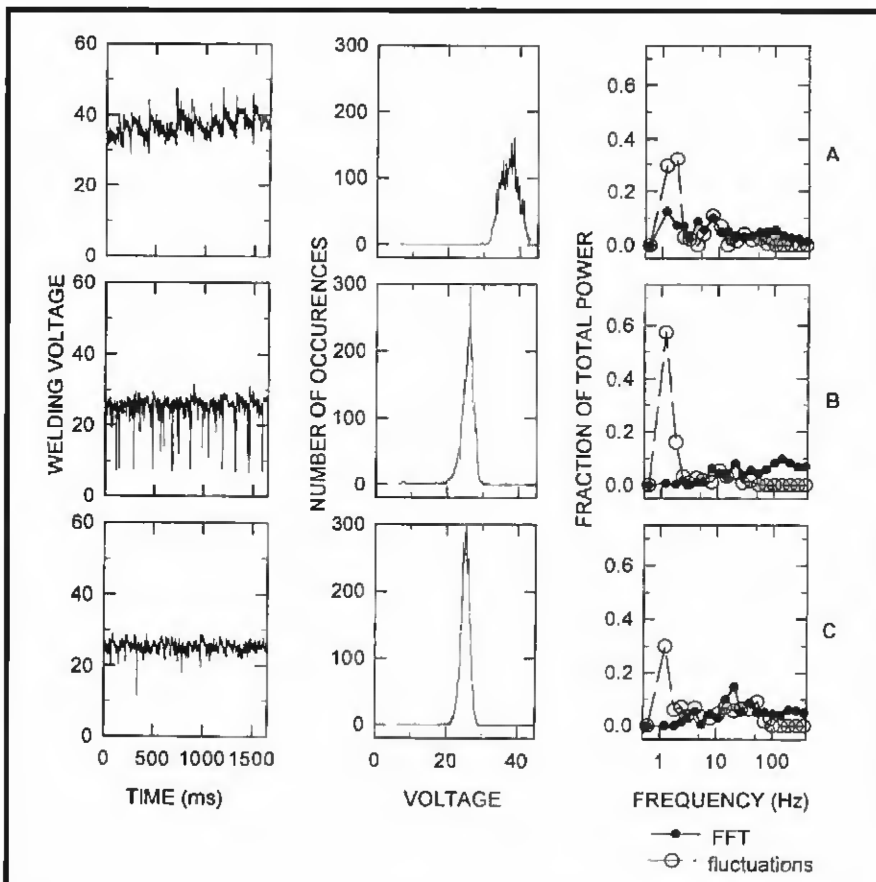

Fig. 8 — The response of a rutile electrode during a bead-on-plate weld. Welding current 128 A; recommended current range 120 to 135 A . A — Behavior during the initial 1.6 s of welding. B — Behavior after approximately 11 s of welding. C — After 35 s. Total arc time, about 40 s.

Characterization of the transfer mode in shielded metal arc welding can be done by droplet collection. The arc signal can be processed in a number of ways. The standard deviation of the

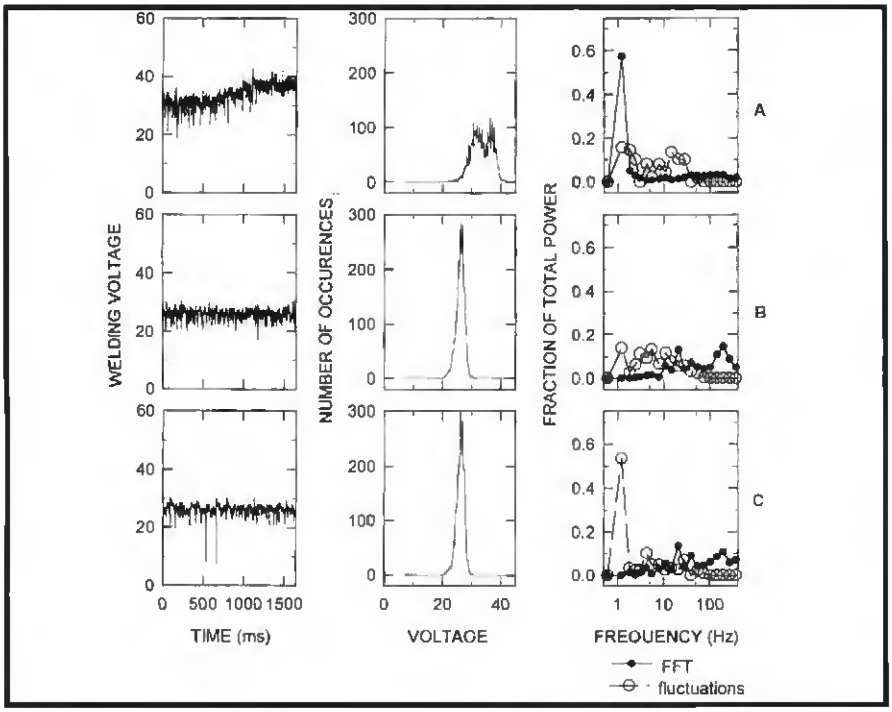

Fig. 9 — The response of a cellulose electrode. Welding current 126 A; recommended current range 100 to 130 A. A — Behavior during the initial 1.6 s of welding. B — Behavior after approximately 11 s of welding. C — After 35 s. Total arc time, about 40 s.

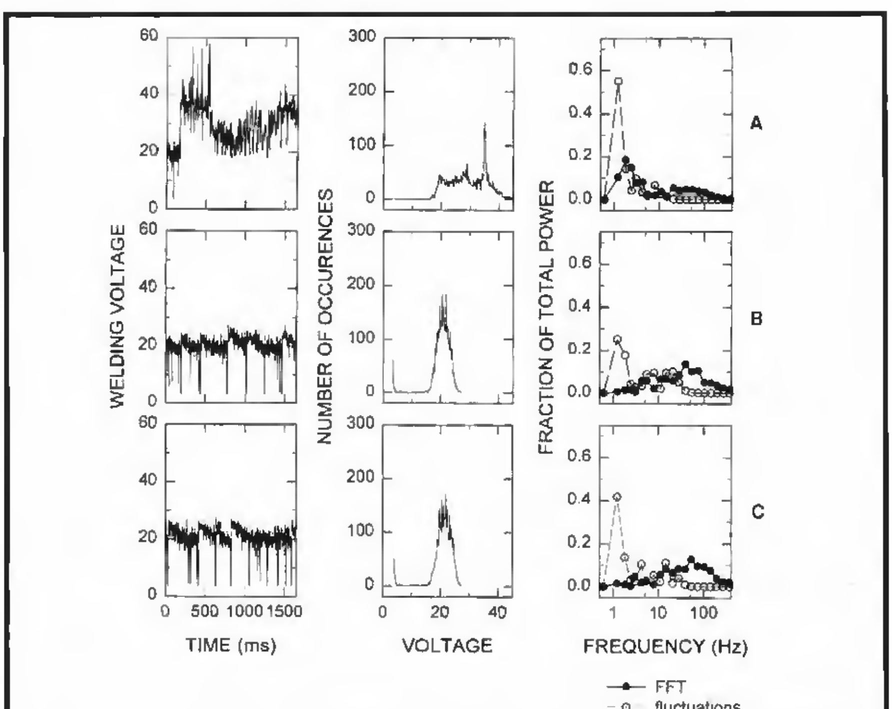

Fig. 10 — The response of a basic electrode. Welding current 141 A; recommended current range 120 to 150 A . A — Behavior during the initial 1.6 s of welding. B — Behavior after approximately 11 s of welding. C — After 35 s. Total arc time, about 40 s.

welding current, or the welding voltage, is not suitable to characterize the transfer mode in shielded metal arc welding.

In the current work, the transfer of droplets was studied for cellulose, rutile, basic electrodes, and a rutile covered stainless electrode. The technique of studying transfer behavior by the correlation of arc signals and droplet measurements is well established for GMAW and FCAW. The objective of this work was to investigate the possible application of this technique to SMAW. In this way, more light was shed on the principles governing the transient nature of metal transfer behavior in the SMAW process.

Experimental Procedure

The transfer mode, and the possible changes in the transfer mode as the electrode was consumed, were characterized for four electrode types: E6010 (cellulose), E6013 (rutile), E7018 (basic), and E309-16 (a rutile covered stainless steel electrode). The electrode diameter was 3.2 mm (1/8 in.). The electrode length was approximately 355 mm (14 in.). A Maxtron 450 inverter-type power supply, switched to the shielded metal arc welding mode, was used. The inductance setting was constant.

The welding voltage was measured between the electrode holder and the workpiece — Fig. 1. The welding voltage signal was used to characterize the transfer behavior, as discussed below. The welding voltage signal was also the input to the arc voltage controller (AVC). As the arc length increased, as the electrode was consumed, the arc voltage and therefore the welding voltage increased. The AVC then, by means of a servo motor, moved the electrode holder downward. The welding voltage was therefore maintained at an approximately constant value. This was done automatically, and continuously, by the AVC, by moving the electrode holder up or down, depending on the deviation between the measured welding voltage and the setpoint. This setpoint was set in the middle of the voltage range recommended by the electrode manufacturer for the specific electrode type. The same setpoint was used for a specific electrode type, regardless of the welding current used. The arc voltage controller did not respond instantaneously to changes in the welding voltage that occurred over a time scale of the order of tens of milliseconds. However, the average welding voltage over a time span of about 500 ms was constant, at the setpoint.

The arc length, and therefore the arc voltage and the measured welding voltage, varied significantly during the brief period associated with arc initiation. The change in welding current associated with a change in welding voltage is determined by the electrical characteristics of the power supply. If the measured welding voltage is plotted against the current, an indication of the power supply characteristics is given — Fig. 2. These characteristics corresponded to those given by the manufacturer of the power supply.

The welding current was varied over a broad range. The angle between the plate and the electrode was maintained at 85 degrees. Bead-on-plate welds were deposited in the horizontal, flat position. A small number of runs with the E6013 electrode was repeated by welding on a water cooled copper tube, as described previously (Ref. 12). The droplets were collected in a horizontal tray fitted with baffles spaced 25 mm apart. The welding speed was maintained at 56 mm/min (2.2 in./min) for the bead-on-plate welds, and at 320 mm/min (12.6 in./min) when welding on the water-cooled copper tube. The droplets were dried, the flux covering was crushed, and the metal droplets magnetically separated from the flux. The size distribution of the droplets was determined by screen analysis, using four screens with aperture sizes of 1168 μm (0.046 in.), 600 μm (0.024 in.), 300 μm (0.012 in.), and 150 μm (0.006 in.). The small mass of the sample between two specific baffles (usually, around 1.0 g) made it impractical to use a larger number of screens for the sieve analysis.

Acquisition of Arc Signals and Subsequent Processing

Both the welding current and the welding voltage were measured and recorded using an analog-to-digital conversion card fitted in a personal computer. The welding current was measured with a Hall effect closed-loop current transducer with a response time of less than 3 μs. The welding voltage was measured between the workpiece and the electrode holder. The arc voltage, the voltage drop along the remaining length of the electrode, and the voltage drop at the contact resistance between the electrode holder and the electrode, therefore, contributed to the welding voltage. Both the welding current and the welding voltage signals were filtered using a simple RC low pass filter with a cutoff frequency of 720 Hz. Filtering the arc signal is essential for successful Fourier transformation of the arc signals. Specifically, the cutoff frequency of the filter should be below the so-called Nyquist frequency.

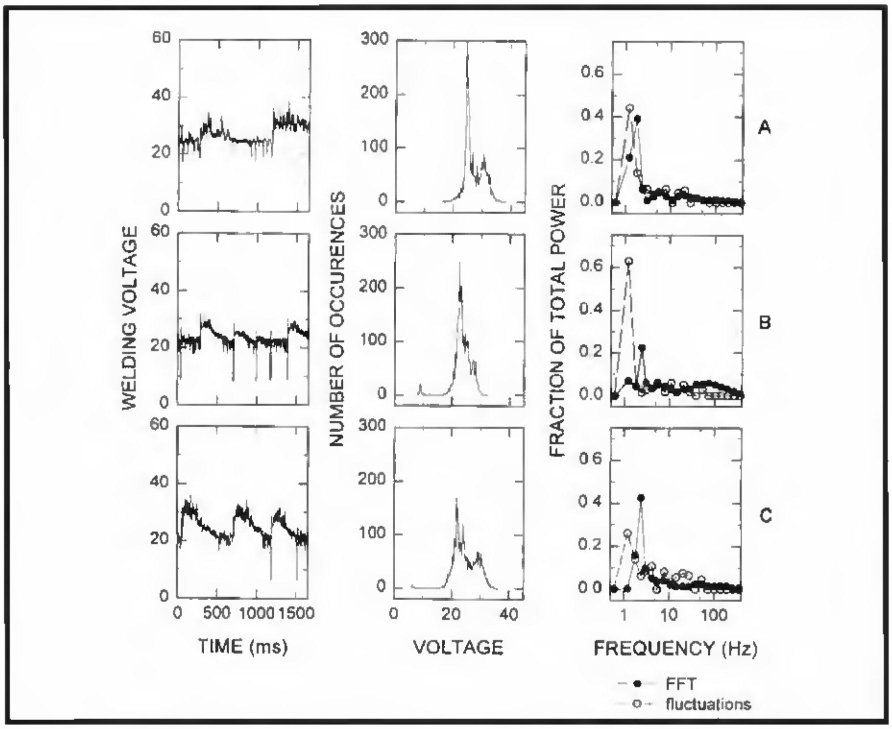

Fig. 11 — The response of a rutile covered type 309 stainless steel electrode. Welding current 101 A; recommended current range 65 to 100 A. A — Behavior during the initial 1.6 s of welding. B — Behavior after approximately 11 s of welding. C — After 35 s. Total arc time, about 46 s.

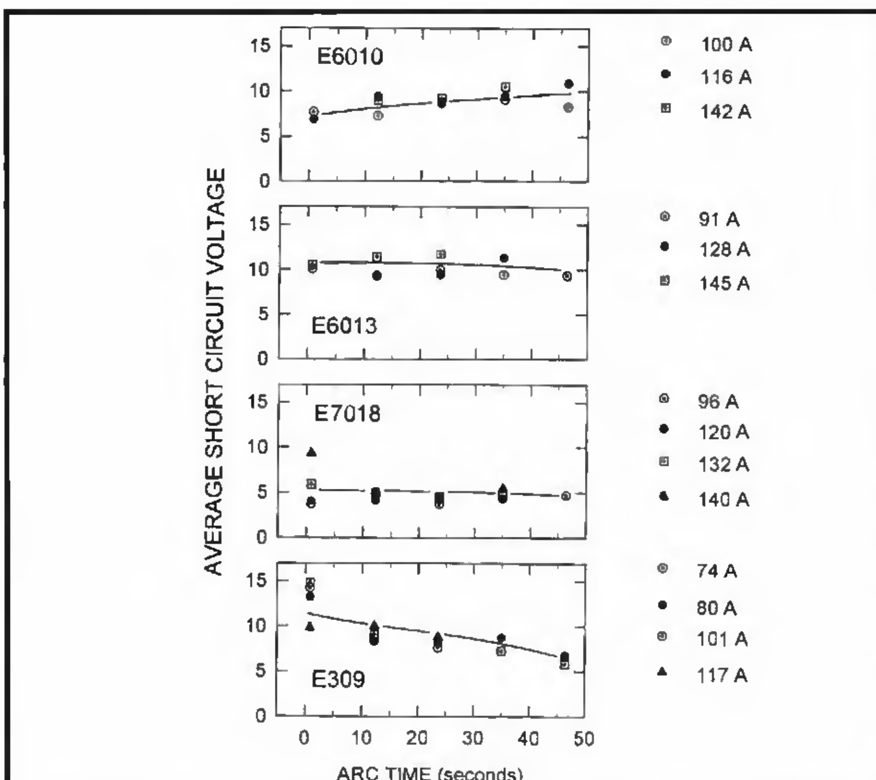

Fig. 12 — The change in the average short circuit voltage, as the electrode is consumed, as a function of the electrode type and the welding current.

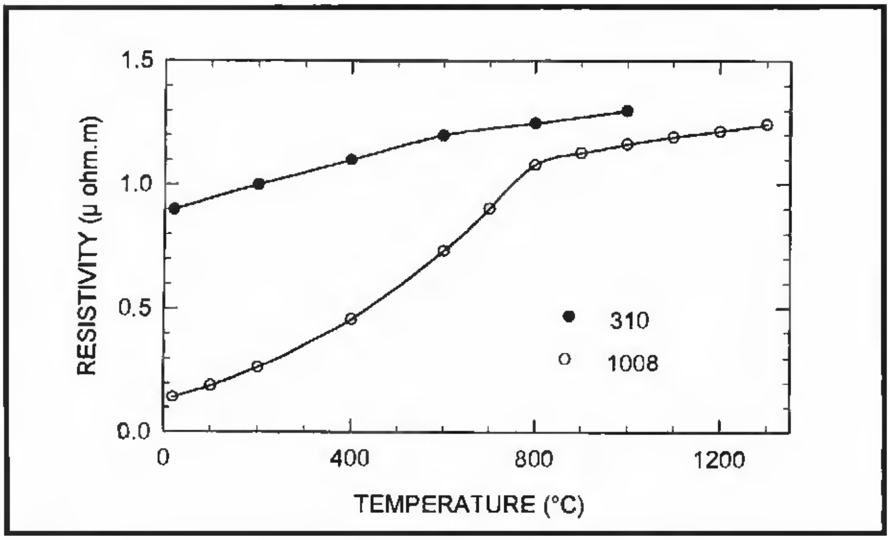

Fig. 13 — Electrical resistivity of low-carbon steel, and austenitic stainless steel with temperature (Refs. 19, 20).

The acquisition frequency of the analog-to-digital conversion card was 2.5 kHz per channel. That means both the welding current and the welding voltage were measured and recorded at 0.4 ms intervals. A total of 8192 measurements (4096 for the current, and 4096 for the voltage) were recorded, covering a period of approximately 1.6 seconds. These data were written to a file on the hard disk of the personal computer. This took considerable time, with the resultant time between measurement periods just under ten seconds. The data acquisition process was repeated until the weld was completed.

The fast Fourier transform of the welding current and the welding voltage signals was done using a previously published algorithm (Ref. 15). The result of this transformation is a record of the power of the signal, as a function of the frequency. (The power of the signal was calculated as the sum of the square of the real and the imaginary parts of the Fourier spectrum at a specific frequency. The power of the signal should not be confused with the electric power of the arc, which is the product of the arc voltage and the welding current.) The resolution for the frequency is given by $1/(N\Delta)$, where N is the number of measurements (in this case, 4096), and Δ is the measurement interval (0.4 ms). The highest frequency which can be characterized by this transformation algorithm is the Nyquist frequency, which is given by $f_n=1/(2\Delta)$ (Ref. 15). In this case, the Nyquist frequency was 1250 Hz, which is well above the cutoff frequency of the RC filter. This would mean that, after fast Fourier transformation of the welding current and the welding voltage signals, both these signals should have a low power in the frequency region from 720 Hz to the Nyquist frequency (1250 Hz).

The algorithm for fast Fourier transform of the welding signals was verified by analyzing a number of signals, and inspecting the results. First, the input signals were generated by a computer program. A single spike resulted in a constant power over the full range of frequencies (Ref. 16). A sine wave with a whole number of cycles was transformed; the result was, as expected, a strong peak at the frequency of the original signal. Second, a signal generator was used to verify the analog-to-digital card and related hardware, the data acquisition software, and the fast Fourier transform algorithm.

Fast Fourier transform of welding signals has been used to characterize the transfer behavior in flux cored arc welding (Ref. 5). FCAW is inherently continuous, and the power – frequency plot is usually dominated by a small number of strong peaks. However, this is not true for shielded metal arc welding. Specifically, a small number of dominant peaks can seldom be identified. If a strong peak on the frequency – power plot originating from the SMAW signal does exist, it may rapidly change to a different frequency, or expand to a number of peaks of lower height. Various explanations exist for this behavior. During shielded metal arc welding, the temperature of the electrode increases, and the transfer behavior changes as the electrode is consumed. This change in the transfer behavior as the electrode is consumed is likely to influence the frequency spectrum. Furthermore, the standard deviation of the power at a specific frequency is always one hundred per cent of the value determined by the fast Fourier transform (Ref. 17). This is normally circumvented by calculating the spectrum from a smaller number of data points than are present in the original signal. The resulting spectra are then averaged at each frequency. The result is a reduction in the variance of the estimate of the power at a specific frequency. Application of this technique to SMAW signals measured during this study did not result in a discernible improvement. A second, related technique, is to conduct a fast Fourier transform of the welding signal, and integrate the resultant power spectrum over a specific frequency range, or ranges. This is similar to an algorithm used to detect contact tube wear during gas metal arc welding, as reported by Quinn, *et al.* (Ref. 18) These workers integrated the power spectral density from 0.3 to 4 Hz. As the contact tube wore, the integral increased.

During this study, the power spectrum was integrated to reflect the activity in a number of frequency ranges. The choice of frequency ranges was guided by inspection of the actual power spectra, and by reference to previous work by Xu (Ref. 19). Xu studied the metal transfer behavior during shielded metal arc welding with E11018, E6013, and E6010 electrodes. Welding with the E11018 electrode was associated with short circuit transfer at 2 Hz. The E6013 electrode exhibited explosive transfer at frequencies in the range of 2 to 6 Hz. The arc signal from E6010 electrode was strong in the 8 to 14 Hz range. Another consideration was the frequency resolution, which was 0.61 Hz during this study. The power spectrum was integrated over multiples of this frequency, which were approximately logarithmically spaced. The maximum frequency was just over 360 Hz, to ensure that the possible influence of the power supply could be characterized. Finally, the integral of the power within a specific frequency interval was expressed as a fraction of the total power over the complete frequency spectrum.

Another way to interpret the welding signal, apart from presenting the data as a histogram, or calculating the power spectrum, is to calculate the fluctuations in voltage or current. As a droplet detaches from the end of the electrode, the arc length increases by a length which can be assumed to be of the order of the diameter of the droplet. The increase in arc length causes an increase in the welding voltage, and a decrease in the current. The size of the fluctuations in voltage and current is calculated by determining the local minima and maxima in the voltage and current signal. The voltage rise is sorted into a specific interval, as is the current drop. The total number of fluctuations falling within a specific range of voltage (or current) can be converted to a characteristic frequency. This is done by dividing the total number of measurements by the measurement time (approximately 1.6 s). Finally, contributions within a frequency range are summed, similarly to the results of the fast Fourier transform, and expressed as a fraction of the total power. The procedure of calculating the fluctuations in voltage or current has two advantages: first, the algorithm for this calculation is considerably shorter than that of the fast Fourier transform; second, the results of the calculations based on the fluctuations in the signal give a more reliable characterization of short circuit transfer. A single short circuit event caused a spike in the voltage and current trace. A fast Fourier transform of a signal consisting of a single spike resulted in a continuous frequency spectrum, which was difficult to interpret.

Using the size of the fluctuations in a signal to calculate a frequency response is a less sophisticated technique than a fast Fourier transform. To give a specific example, consider three signals: a sine wave, a triangular wave, and a square wave, all with the same fundamental frequency, and the same amplitude. A fast Fourier transform of these signals would yield the same fundamental frequency, but different powers at higher frequencies (the higher harmonics of the signal). To use the fluctuation in the signal, as proposed above, would yield the same result for the three different signals. This does not present a serious objection. The transfer behavior during arc welding is usually characterized by the fundamental frequency, not the shape of the waveform of the arc signal. A recent study of the plasma parameters in gas metal arc welding is an exception (Ref. 20). In that study, the rise rates of the voltage and current during droplet detachment were used to establish the electron temperature distribution.

Results and Discussion

Power Supply Characteristics

The dynamic voltage – current characteristic of the power supply, as determined during welding, is shown in Fig. 2. The relationship between the voltage and the current exhibited fairly complex behavior. However, most of the time, the welding voltage was a linear function of the current. For a welding current of 150 A, there was a straight line between 29 V, 90 A, and 20 V, 175 A — Fig. 2. At currents above 175 A, the welding voltage can be one of two discrete values; these values probably corresponded to stubbing, and the short circuit condition. Welding at a lower current setting resulted in an essentially similar voltage – current characteristic, the only change being that the welding voltage – welding current function was shifted horizontally. The characteristics of the power supply, and specifically the straight line with a finite slope, implied that either the voltage or the current could be used to characterize the transfer behavior.

The open circuit voltage was above 60 V — Fig. 2. The range of the welding voltage with an open circuit was approximately 1 V — Fig. 3. The power spectrum of this signal is shown in Fig. 4A. The power spectrum is dominated by peaks at the line frequency (60 Hz) and at multiples of this frequency. The initial interpretation would be that any variation in the welding voltage of less than 1 V was due to electrical noise emanating from the power supply. Close inspection of the power spectra of signals generated during welding showed the height of the peaks at 60 Hz and its multiples to be considerably lower than in the case of the open circuit condition — Fig. 4B. Ignoring all voltage fluctuations below 1 V also did not significantly change the frequency spectrum, as calculated from the fluctuations in the welding voltage. During welding, a heavy current flows. The inductance in the circuit limits the rate of change of the welding current, and the voltage and the current cannot vary independently — Fig. 2. Therefore, even small variations in the welding voltage, as measured during welding, were due to transfer events, and not the line frequency.

Characterization of Transfer Behavior

In Fig. 5 and Figs. 8–11, the change in transfer behavior during specific electrode consumption was characterized by presenting the results of four different signal processing techniques. First, the change in the welding voltage with time was shown. Second, the histogram of the welding voltage, that is, the number of times the welding voltage was measured in a certain interval, was shown. Finally, the frequency response of the welding voltage is shown. The frequency response was calculated using two techniques. The results of the fast Fourier transform were integrated over a limited number of frequency ranges (as discussed previously). Also, the frequency response was calculated from the size of the individual fluctuations in the welding voltage. These results, that is, the welding voltage, the histogram of the welding voltage, and the frequency response of the welding voltage, are shown at three different times as the electrode is consumed, usually during the first 1.6 s of welding, after approximately 11 s of welding, and 35 s after the arc was initiated. The total arc time varied between 35 and 46 s.

E6013 (Rutile) Electrodes

Rutile electrodes were used for bead-on-plate and nonfusion welds. The recommended current range for the electrodes used is 120 to 135 A (15.2 to 17.1 A/mm^2). The current for the bead-on-plate welds varied from 91 to 146 A (11.5 to 18.4 A/mm^2). For the nonfusion welds, the corresponding figure is 122 to 144 A (15.4 to 18.2 A/mm^2). Welding on a water-cooled copper tube was characterized by a number of large and rapid fluctuations in the welding voltage, after the initial transient — Fig. 5B. Each of these fluctuations is associated with a short circuiting event. The number of these events seemed to decrease as the electrode was consumed — Fig. 5C. The decrease in short circuit transfer is also evident in the size distribution of the droplets captured during nonfusion welds — Fig. 6. The mass fraction of droplets with a nominal size larger than 1168 μm (0.046 in.) decreased as the electrode was consumed. It seems reasonable to assume that the formation of a large droplet, and its detachment from the tip of the electrode, is associated with the large and rapid fluctuations observed in the welding voltage. The reduction in droplet size occurring as the electrode is consumed is also illustrated by scanning electron microscope images of some of the droplets collected during welding with a rutile electrode on a water-cooled copper tube — Fig. 7.

During the earlier stages of a fusion weld, the power spectrum exhibits peaks over a broad range of frequencies, up to about 150 Hz — Fig. 8. This is true regardless of the welding current, or whether the substrate is a steel plate or a water-cooled copper tube. At longer arc times, especially if a higher welding current is used, the number of short circuit events decreases, as was the case for the nonfusion welds. The number of short circuit events is considerably smaller for nonfusion welding, which constitutes the major influence the substrate has on the transfer behavior of rutile electrodes.

The average welding voltage, as set for the automatic voltage controller, was the same for bead-on-plate welds and nonfusion welds. As a first approximation, the arc length would therefore be same, whether a weld pool was present or not. Movement of the weld pool might therefore play an important role in the formation of a short circuit.

The welding voltage histogram may initially be fairly broad. As the electrode is consumed, the distribution of welding voltage becomes more narrow. This is probably related to the decrease in the number of short circuit events. The decrease in the width of the welding voltage distribution is more pronounced if the welding current is higher. If the welding current is too low (96 A), a large number of short circuit events occurs. Short circuit transfer is diminished and fine droplet transfer is augmented as the electrode is consumed. However, in the case of rutile electrodes, the high-frequency peak that develops is not as well defined as for cellulose electrodes.

E6010 (Cellulose) Electrodes

The recommended current range for the cellulose electrodes is 100 to 130 A, which corresponds to a current density between 12.6 and 16.4 A/mm^2. The actual current used to weld these electrodes ranged from 100 to 147 A (12.6 to 18.6 A/mm^2). On the power spectrum established by fast Fourier transform of the welding voltage, some activity existed around 10 Hz, especially early during welding with a current of 126 A — Fig. 9. The frequency response calculated from the fluctuations in the welding voltage also showed this behavior, indicating that some short circuit events did occur. Short circuiting seemed to diminish as the electrode was consumed. A broad range of peaks was present above 100 Hz, if a high current was used. These peaks diminished in intensity as the electrode was further consumed. This decrease of peaks above 100 Hz was more intense as the welding current is increased — Fig. 9. An increase in current from 126 A (which is just below the highest recommended current) to a level exceeding the maximum current specified by the electrode manufacturer did not change this behavior significantly. At lower currents, the welding voltage signal never developed a strong response above 100 Hz. The voltage distribution — as exemplified by a histogram — is generally narrow, although it may be bimodal during arc initiation. The width of the histogram seems to become narrower as the electrode is consumed; this tendency is stronger at a higher welding current. Charring of the electrode covering was observed during welding at a high current. This means that the flux gives off a considerable amount of CO_2 away from the arc. The associated decrease in the CO_2 content of the arc atmosphere causes an increased activity at higher frequencies, which is probably indicative of fine droplet transfer. This would indicate that, as a cellulose electrode is consumed, the dominant transfer mode becomes a fine droplet transfer. This may be the result of a decrease in the CO_2 content of the arc atmosphere.

E7018 (Basic) Electrodes

The recommended current for the basic electrodes was 120 to 150 A (15.2 to 18.9 A/mm^2). The actual welding current ranged from 96 A (12.1 A/mm^2) to 150 A. Transfer behavior was dominated by short circuit transfer. The histogram of the welding voltage reflected this, with a strongly bipolar distribution — Fig. 10. The lower peak on the histogram corresponded to short circuit mode. Even the higher peak of the bimodal distribution was considerably broader than the peak on the histogram for either the cellulose or the rutile electrode. The second peak on the voltage distribution for the basic electrode was much broader if the welding current was low.

If the welding current falls within the recommended range, the power spectrum develops significant activity in the region of 40 Hz, as the electrode is consumed. Short circuit transfer is not diminished as the electrode is consumed, as can be seen from the height of the peak in the frequency response calculated from the fluctuations in the welding voltage. The activity around 40 Hz develops earlier if the welding current is higher. It is reasonable to assume that this phenomenon is related to heating of the flux.

Rutile Covered Stainless Steel Electrodes

The manufacturer recommended that these electrodes be welded with a current between 65 and 100 A (8.2 to 12.6 A/mm^2). The current used during this study ranged from 74 to 118 A (9.3 to 14.9 A/mm^2). The power spectrum was dominated by a single peak at a low frequency. This peak initially occurred at 1.8 Hz, and shifted to 2.4 Hz as the electrode was consumed. This was demonstrated by both the results of the fast Fourier transform and the calculations based on the voltage fluctuations — Fig. 11. The correlation between these two estimates of the power spectrum was good, the best for all the electrodes characterized during this study. This was probably the fortuitous result of the fact that the dominant frequency was well above the frequency resolution (0.61 Hz). The shift in the peak frequency as the electrode was consumed, occurred for a welding current from about 80 A to 118 A. The shift occurred slightly earlier during the weld if the welding current was higher. This electrode shows the lowest sensitivity to changes in the welding current of the four different electrode types characterized during this study.

Validity of the Use of the Welding Voltage

The welding voltage, as measured in this study, is made up of the arc voltage, the voltage drop along the remaining length of the electrode, and the voltage drop at the contact resistance between the electrode holder and the electrode. The voltage drop along the length of the electrode — the electrode voltage — is not expected to stay constant as the electrode is consumed. As a first approximation, this is not expected to influence the use of the welding voltage to interpret the transfer behavior, because of its gradual increase as the electrode is consumed (Ref. 12). This change will occur over the total arc time, which is in the order of 40 s, and should therefore not have any significant influence on the frequency response of the welding voltage. It may, however, have a major influence on the shape of the welding voltage histogram. This effect was evaluated by calculating the average welding voltage during short circuit events, as the electrode is consumed — Fig. 10. During a short circuit, the welding voltage drops to the sum of the voltage drop along the remaining length of the electrode and the voltage drop at the contact resistance between the electrode and the electrode holder. For type E6010, E6013, and E7018 electrodes, this short circuit voltage did not change significantly with welding current, or with the total arc time. This can be explained by the fact the average temperature of the remaining length of the electrode increases as the electrode is consumed. The associated increase in electrical resistivity seems to largely compensate for the decreasing length of the electrode. The result is that the voltage drop along the remaining length of the electrode, and therefore the short circuit voltage, stays approximately constant as the electrode is consumed — Fig. 12.

The average short circuit voltage during welding with an austenitic stainless steel electrode does not stay constant. For these electrodes, the short circuit voltage shows a consistent decrease. This may be explained by the change in electrical resistivity as a function of temperature — Fig. 13. While the electrical resistivity of an austenitic steel (Ref. 21) is considerably higher than that of a ferritic steel (Ref. 22) at room temperature, the increase in resistivity with temperature is smaller for an austenitic steel than for a ferritic steel. This means that the increase in temperature does not compensate for the decrease in length of the E309 electrode, and the short circuit voltage drops consistently. The fact that the transfer behavior of the austenitic stainless steel electrodes is less sensitive to the welding current than that of the low carbon steel electrodes may be related to the change in electrical resistivity with temperature. Even a relatively low welding current may cause significant ohmic heating of the electrode, with the associated changes in the transfer behavior.

Final Remarks

The objective of this work was primarily to study the transfer behavior of SMAW electrodes. The change in transfer behavior as the electrode is consumed, and that this change is larger if the welding current is higher, point to the practical danger of using a welding current higher than the maximum current recommended by the electrode manufacturer.

The transfer behavior of the stainless electrode used in this study showed the smallest change as the electrode was consumed. The transfer behavior of this electrode type also had the lowest sensitivity to changes in the welding current. This could be because the resistivity of austenite is much less sensitive to temperature than the resistivity of ferrite (Fig. 13), or it could be due to the inherent characteristics of the flux covering of the stainless electrode. This issue presents an avenue for future work, to compare the transfer behavior of a stainless electrode with an austenite core rod with that of a stainless electrode with a ferritic core rod.

Conclusions

1) The transfer of droplets during shielded metal arc welding on a water-cooled copper tube was different from the transfer from the same electrode type, at the same welding current, during fusion welding. Specifically, the number of short circuiting events was considerably smaller during welding on a copper tube.

2) Processing of the welding voltage signal could be done in different ways to characterize the transfer behavior during shielded metal arc welding. The histogram of the welding voltage provided a useful visual summary of the behavior of the arc. The welding voltage signal could also be processed by a fast Fourier transform, or by calculating the frequency response from the size of the individual fluctuations in the welding voltage.

3) The transfer behavior of cellulose electrodes (E6010), rutile electrodes (E6013), and basic electrodes (E7018) all changed significantly as the electrode was consumed. These changes were more pronounced if the welding current was higher.

4) The transfer behavior of the cellulose, rutile, and basic electrodes differed substantially. Specifically, welding with a basic electrode was characterized by a substantial number of short circuit events. As a basic electrode was consumed, more short circuiting occurred, and the size of the droplets increased. During the welding of a rutile electrode, the average size of the droplets decreased, and the number of short circuiting events decreased.

5) Of the four electrodes studied, the transfer behavior of the stainless electrode showed the smallest changes as the electrode was consumed. This electrode also had the lowest sensitivity to changes in the welding current. As the electrode was welded, a small shift to higher frequencies occurred.

Acknowledgements

The financial support of Eskom TRI for one of the authors (P. G. H. Pistorius) is gratefully acknowledged.

References

1. Heald, P. R., Madigan, R. B., Siewert, T. A., and Liu, S. 1994. Mapping the droplet transfer modes for an ER100S-1 GMAW electrode. *Welding Journal* 73(2): 38-s to 44-s.

2. Modenesi, P. J., and Nixon, J. H. 1994. Arc instability phenomena in GMA welding. *Welding Journal* 73(9): 219-s to 224-s.

3. Jönsson, P. G., Szekely, J., Madigan, R. B., and Quinn, T. P. 1995. Power characteristic in GMAW: experimental and numerical investigation. *Welding Journal* 74(3): 93-s to 102-s.

4. Amson, J. C. 1972. Electrode voltage in the consumable-electrode arc system. *Journal of Physics. D: Applied Physics.* 5: 89 to 96.

5. Wang, W., Liu, S., and Jones, J. E. 1995. Flux cored arc welding: arc signals, processing, and metal transfer characterization. *Welding Journal* 74(11): 369-s to 377-s.

6. Stern, I. L., 1948. Overheating of electrodes. *Welding Journal* 27(7): 522 to 526.

7. Ter Berg, J., and Larigaldie, A. 1952. Melting rate of coated electrodes. *Welding Journal* 32(5): 268-s to 271-s.

8. Waszink, J. H., and Piena, M. J., 1985. Thermal processes in covered electrodes. *Welding Journal* 64(2): 37-s to 48-s.

9. Chen, J. H., and Kang, L. 1989. Investigation of the kinetic process of metal-oxygen reaction during shielded metal arc welding. *Welding Journal* 68(6): 245-s to 251-s.

10. Pokhodnya, I. K., Gorpenyuk, V. N., Milichenko, S. S., Ponomarev, V. E., Starodubtsev, L. V., Shvachko, V. I., and Yavdoshchin, I. R. 1991. *Metallurgy of Arc Welding.* Vol. 1: Arc Processes and Electrode Melting, Riecansky Science Publishing Co., Cambridge, U.K. 173 to 222.

11. *Ibid.* p. 68.

12. Brandi, S., Taniguchi, C., and Liu, S. 1991. Analysis of metal transfer in shielded metal arc welding. *Welding Journal* 72(12): 529-s to 536-s.

13. Bracarense, A. Q., and Liu, S. 1993. Chemical composition variations in shielded metal arc welds. *Welding Journal* 72(12): 529-s to 536-s.

14. Bracarense, A. Q., and Liu, S. 1994. Control of covered electrode heating by flux ingredients substitution. *Welding and Metal Fabrication* 62(5): 224 to 229.

15. Press, W. H., Teukolsky, S. A., Vetterling, W. T., and Flannery, B. P. 1992. Numerical Recipes in C. The Art of Scientific Computing. Second Edition, Cambridge University Press, Cambridge, U.K. 497 to 512.

16. Wang, W. 1991. A methodology for the study of metal transfer modes in flux cored arc welding. Colorado School of Mines, M. S. Thesis.

17. Press, W. H., *et al.*, *Ibid.*, p. 552.

18. Quinn, T. P., Madigan, R. B., Morris, M. A., and Siewert, T. A., 1995. Contact tube wear detection in gas metal arc welding. *Welding Journal* 74(4): 115-s to 121-s.

19. Xu, X., 1994. Study of metal transfer modes in shielded metal arc welding. Colorado School of Mines, M. S. Thesis T-4352.

20. Nemchinsky, V. A. 1994. Plasma parameters near a small anode in a high pressure arc (gas metal arc welding). *Journal of Physics D: Applied Physics.* 27: 2515–2521.

21. Davis, J. R., *et al.* 1994. ASM *Specialty Handbook.* Stainless Steels. ASM International. p. 491.

22. Davis. J. R., *et al.* 1990. *Metals Handbook* Tenth Edition. Vol. 1. Properties and Selection: Irons, Steels, and High-Performance Alloys. ASM International. p. 189.